Delft University of Technology

Design drivers for the storage system of baseload hybrid power plants

Iori, J.; Zaaijer, M B; von Terzi, D.A.; Watson, S.J.

DOI
10.1049/icp.2024.1844

Publication date
2024

Document Version
Accepted author manuscript

Published in
8th International Hybrid Power Plants and Systems Workshop, HYB 2024

Citation (APA)
Iori, J., Zaaijer, M. B., von Terzi, D. A., & Watson, S. J. (2024). Design drivers for the storage system of baseload hybrid power plants. In *8th International Hybrid Power Plants and Systems Workshop, HYB 2024* (2 ed., Vol. 2024, pp. 245-250) https://doi.org/10.1049/icp.2024.1844

Important note
To cite this publication, please use the final published version (if applicable).
Please check the document version above.

Copyright
Other than for strictly personal use, it is not permitted to download, forward or distribute the text or part of it, without the consent of the author(s) and/or copyright holder(s), unless the work is under an open content license such as Creative Commons.

Takedown policy
Please contact us and provide details if you believe this document breaches copyrights.
We will remove access to the work immediately and investigate your claim.

This work is downloaded from Delft University of Technology.
For technical reasons the number of authors shown on this cover page is limited to a maximum of 10.

DESIGN DRIVERS FOR THE STORAGE SYSTEM OF BASELOAD HYBRID POWER PLANTS

Jenna Iori[1]* , Michiel Zaaijer[1], Dominic von Terzi[1], Simon Watson[1]

[1] Faculty of Aerospace Engineering, TU Delft, Delft, Netherlands
**j.iori@tudelft.nl*

Keywords: HYBRID POWER PLANT, BASELOAD POWER PRODUCTION, LONG-TERM STORAGE, WIND

Abstract

For scenarios of high penetration of renewable energy, it becomes increasingly relevant to improve the dispatchability of supply for wind and solar power plants. Baseload power plants, required to produce a minimum power production at all times, are discussed in this context. The baseload constraint can be satisfied with renewable sources when combined with a storage system but at a high cost. This work studies the design drivers of such a storage system when consisting of short and long-term storage. The capacities of the short-term and long-term storage components are calculated as part of a linear optimization problem with the objective of minimizing the cost of baseload, using a metric based on a net present value formulation. Our analysis, based on 10 locations in Northern Europe, highlights a high sensitivity of optimal storage sizing to storage cost assumptions. In addition, the cost of baseload is found to be correlated to the share of renewable power produced above baseload, but not to the correlation between price and wind power, suggesting arbitrage plays a minor role in the business case.

1 Introduction

An important challenge of renewable generation is how to manage its weather dependence. For scenarios of high penetration of renewables, there is a risk of not supplying power during days of low wind or solar availability. As such, there is increased interest in improving the dispatchability of renewable energy sources, i.e. their ability to produce power on demand regardless of weather conditions. One of the tender criteria for the Dutch wind farm Hollandse Kust Noord was to develop innovations for supply flexibility in offshore wind farms [1]. Dispatchability can be achieved on a short time scale by using a storage system to compensate for the error in power production due to an imprecise forecast [2–4]. Another example of dispatchability is a power plant providing baseload power regardless of the weather conditions. Baseload power production can be provided with renewable energy, using concentrated solar power [5] or storage systems combined with a wind-solar PV hybrid power plant [6].

However, providing baseload power requires a large energy storage capacity, which tends to be expensive for established short-term storage (STS) technologies such as lead-acid (LEAD) and lithium-ion batteries (LIB). The alternative is to use long-term storage (LTS) systems, such as pumped-storage hydropower (PSH) or compressed air energy storage (CAES), which tend to have a low marginal cost for energy storage, but a high cost for power capacity. A combination of STS and LTS is likely to be adequate to satisfy the baseload constraint, where the proportion of each storage type depends on its techno-economic properties. When it comes to costs, there is a large diversity among existing technologies, as shown in Fig. 1 with data from [7]. There is also uncertainty in future costs for technologies in development such as gravity storage (G), pumped

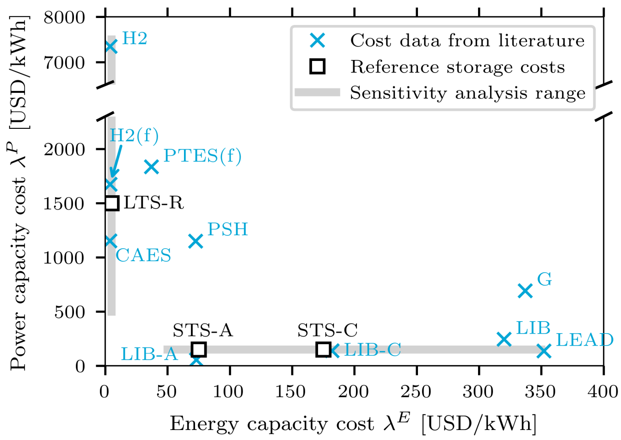

Fig. 1 Energy and power capacity storage costs used in this work (reference values and ranges) compared to the data from [7]. Projected future costs are indicated with (f). The meaning of the suffixes A and C is explained in Section 3.

thermal energy storage (PTES) or hydrogen storage combined with electrolyzers and fuel cells (H2). As such, it is particularly relevant to understand how a cost variation impacts the storage system sizing. In this context, we address the following research questions:

- What is the optimal balance between STS and LTS to satisfy baseload power production at minimal cost?
- What is the sensitivity of the sizing and total cost to storage cost assumptions and site characteristics?

Our study focuses on the storage sizing problem for a hybrid wind-storage power plant required to produce baseload power.

2 Model and optimization problem

2.1 Storage system model

The storage system is modelled as a combination of short-term storage (STS) and long-term storage (LTS), indicated by the subscript $j = 1, 2$, respectively. Each storage type is described by its energy capacity $\bar{E}_j$, power capacity $\bar{P}_j$ and round-trip efficiency η_j, as well as its power and energy level over time, $\boldsymbol{P}_j$ and $\boldsymbol{E}_j$, for $j = 1, 2$. The storage losses are taken into account during discharge. We use the convention of positive power for discharge, and negative power for charge. As a result, the operation of each storage type can be modelled by three equations describing (i) the relation between power and energy during charge and discharge, (ii) the limit on storage power related to its power capacity and (iii) the limit on stored energy related to the energy capacity. They are represented below:

$$E_j^{t+1} - E_j^t = \begin{cases} -\Delta t P_j^t & \text{if } P_j^t \leq 0 \\ -\dfrac{\Delta t}{\eta_j} P_j^t & \text{else} \end{cases} \qquad t = 1, .., n, \qquad (1)$$

$$-\bar{P}_j \leq P_j^t \leq \bar{P}_j \qquad t = 1, .., n, \qquad (2)$$

$$0 \leq E_j^t \leq \bar{E}_j \qquad t = 1, .., n+1, \qquad (3)$$

where the superscript $\square^t$ is to used to indicate the time step, Δt refers to the time step duration and n is the number of time steps with $\boldsymbol{P}_j \in \mathbb{R}^n$ and $\boldsymbol{E}_j \in \mathbb{R}^{n+1}$, for $j = 1, 2$.

2.2 Cost of baseload

We use the term *cost of baseload* to represent the financial burden of satisfying a baseload constraint during the project lifetime. This metric represents the difference between the Net Present Value (NPV) for the wind farm with and without a baseload constraint. It is calculated from the overnight capital cost of the storage system and the possible revenues obtained by arbitrage on the day-ahead market, with electricity prices denoted by $\boldsymbol{\lambda}_{\text{DAM}}$. The cost of baseload is a function of the design variables $\boldsymbol{x} = [\boldsymbol{P}_1, \boldsymbol{P}_2, \boldsymbol{E}_1, \boldsymbol{E}_2, \bar{P}_1, \bar{P}_2, \bar{E}_1, \bar{E}_2]^T$:

$$c(\boldsymbol{x}) = \sum_{j=1}^{2} \frac{m}{m_j} (\lambda_j^P \bar{P}_j + \lambda_j^E \bar{E}_j) - \sum_{k=1}^{m} \frac{\boldsymbol{\lambda}_{\text{DAM}}^T (\boldsymbol{P}_1 + \boldsymbol{P}_2)}{(1+r)^k}, \qquad (4)$$

where $\square^T$ represents the transpose operator, and λ_j^E, λ_j^P are the cost per energy and power capacity, respectively. The lifetime of the storage type m_j relative to the project lifetime m is taken into account to represent possible replacements. Both m and m_j are expressed in years. We use r as the real interest rate instead of the discount rate in order to take in account the inflation in the calculation, here assumed constant over the project duration.

2.3 Integrated sizing optimization

The storage system is sized using a linear program with the objective to minimize the cost of baseload c while satisfying a baseload power constraint with a reliability of 99%, represented by the vector $\boldsymbol{P}_{\text{min}}$. The time steps where the baseload production is required are fixed before the optimization. The energy and power capacity for each storage type, as well as their hourly operation for one year, are considered as design variables. Constraints are enforced to ensure that (i) the total power produced, considering the wind farm production $\boldsymbol{P}_{\text{WF}}$, satisfies the baseload constraint and does not exceed a maximum bound $\boldsymbol{P}_{\text{max}}$, (ii) the storage energy levels are equal at the start and end of the year, and (iii) the storage model is respected (Eq. 1-3). The following problem formulation is obtained:

$$\begin{aligned} \min_{\boldsymbol{x}} \quad & c(\boldsymbol{x}) & & \\ \text{s.t} \quad & \boldsymbol{P}_{\text{min}} - \boldsymbol{P}_{\text{WF}} \leq \boldsymbol{P}_1 + \boldsymbol{P}_2 \leq \max(\boldsymbol{0}, \boldsymbol{P}_{\text{max}} - \boldsymbol{P}_{\text{WF}}) & & \\ & E_j^1 = E_j^{n+1}, & & j = 1, 2 \\ & E_j^{t+1} - E_j^t \leq -\Delta t P_j^t \qquad t = 1, .., n & & j = 1, 2 \\ & E_j^{t+1} - E_j^t \leq -\frac{\Delta t}{\eta_j} P_j^t \qquad t = 1, .., n & & j = 1, 2 \\ & \text{Eq. (2-3)} & & j = 1, 2 \end{aligned} \qquad (5)$$

Equation 1 is included in the problem formulation in a relaxed form, in order to maintain a linear formulation. While this choice is less common than a mixed-integer linear formulation, it has been used in energy system design studies [8, 9] and allows the computational burden to be decreased by several orders of magnitude. The linear program is solved using MOSEK [10]. Figure 2 shows an example of storage operation with optimal design. The difference in operation between

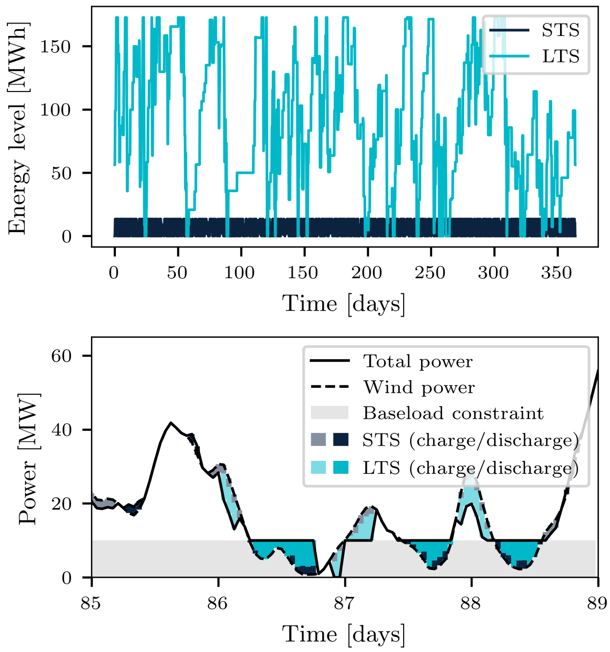

Fig. 2 Optimal operation strategy for the reference case to satisfy a 10 MW baseload constraint in terms of energy levels and power production, using STS-A and LTS-R.

the two storage types is correctly captured, where STS tends to operate at a higher frequency than LTS. In addition, the contribution of the storage types to the baseload is shown. At the end of day 86, the power shifts from the 10 MW baseload to 0 MW, illustrating the 99% reliability.

3 Case studies

The sizing methodology is applied to several test cases, with different storage cost assumptions and site characteristics. We use one reference for the LTS (LTS-R) and two for the STS, listed in Table 1 and represented in Fig. 1. They are not associated with specific technologies but are used as an abstract representation of long and short-term storage systems. The two reference STS systems correspond to different costs, adapted from the cost assumption for utility-scale batteries in 2050 described in [7]. STS-C assumes a conservative evolution of the costs, whereas STS-A uses an advanced scenario which leads to lower costs. The wind power production is calculated using the Renewables.ninja platform*, based on a global reanalysis dataset, and a virtual wind farm model [11, 12]. Wind power production time series are extracted for a 100 MW wind farm for 10 offshore locations in Nothern Europe shown in Fig. 3, and using three different wind turbine technologies listed in Table 2. This results in 30 cases, with the *reference case* corresponding to the location of Hollandse Kust Noord with turbine technology A. The price time-series are obtained from ENTSO-E [13] with a pass-band filter to remove extreme events. Data are extracted for 2019. Furthermore, we use a project duration of 20 years, a 3 % real interest rate and a maximum power of 100MW.

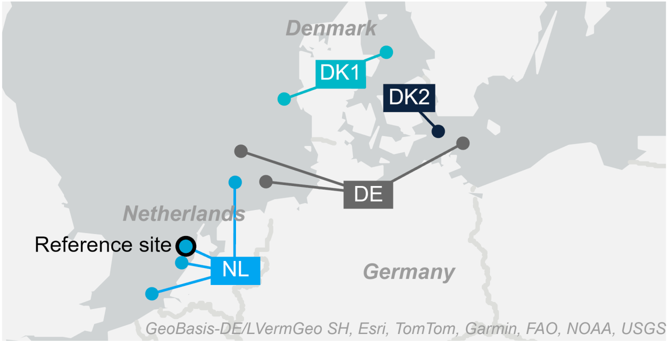

Fig. 3. Site locations and associated energy market zones.

Table 1 Characteristics of the three reference storage systems

	STS-A	STS-C	LTS-R
Energy capacity cost [USD/kWh]	75	175	5.0
Power capacity cost [USD/kW]	150	150	1500
Round trip efficiency [%]	85	85	50
Lifetime [years]	10	10	20

Table 2 Characteristics of the three wind turbine technologies

Technology	A	B	C
Hub height [m]	80	135	140
Rotor diameter [m]	130	126	164
Rated power [MW]	4.0	6.5	8.0

4 Results

4.1 Drivers for the optimal storage sizing

We first study the optimal storage sizing across test cases and for different baseload levels. Several conclusions can be drawn from our results, based on Fig. 4. A higher baseload level increases the total energy capacity but lowers the share of STS in the total energy and power capacity. Indeed, the LTS becomes more relevant due to its low energy capacity cost when the baseload increases and the energy requirement with it. Thus, there is more investment in LTS even though the LTS power capacity cost is 10 times higher than for STS. Furthermore, the data shows that the total power capacity is equal or below the baseload level for the conservative STS costs assumption. In contrast, there is a tendency to oversize the storage when the STS is cheaper (STS-A), suggesting that the storage system is used for arbitrage. We note that there is a large variation in total power and energy capacity overall, and the share of STS, suggesting that the optimal sizing is sensitive to the specific site characteristics.

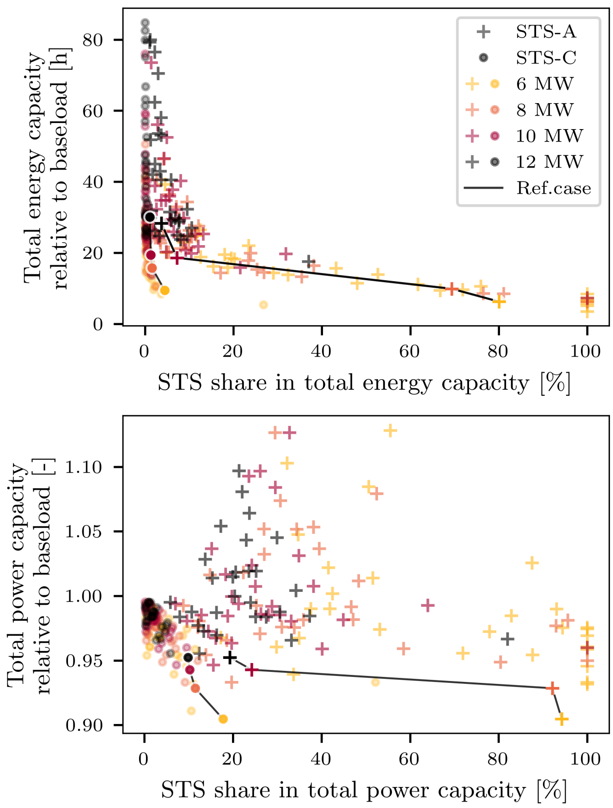

Fig. 4 Impact of baseload level on optimal storage sizing, for all case studies and for two STS cost assumptions and LTS-R. The data for the reference case is highlighted with black lines.

*www.renewables.ninja

The influence of the STS energy capacity cost is reported in more detail in Fig. 5. The total power capacity is insensitive to the storage costs above a certain threshold (around 100 USD/kWh). Below this threshold, the tendency to size the storage above the baseload level is confirmed. However, no trend appears in terms of energy capacity, which indicates a larger impact of site characteristics. Finally, there is a large variation of sizing between the two cost assumptions STS-A and STS-C, suggesting that the uncertainty on future costs is likely to translate into uncertainty on the optimal storage sizing.

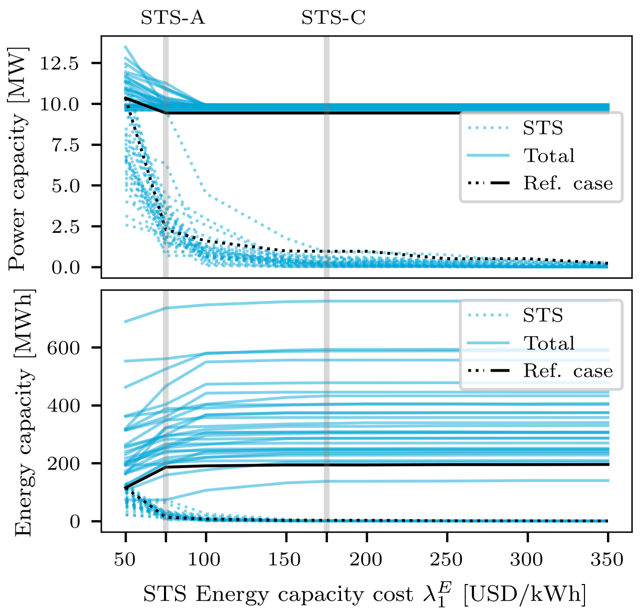

Fig. 5 Impact of a variation of STS energy capacity costs on the optimal sizing, for all case studies and using the reference long-term storage (LTS-R). The data for the reference case are highlighted in black.

4.2 *Cost of baseload sensitivity to storage costs*

We further analyse the impact of LTS and STS storage cost assumptions on the cost of baseload. This is done by varying the LTS power capacity cost and the STS energy capacity cost, over ranges represented in Fig.1. These two metrics are used since they are dominating the costs of the two types of storage. The other two cost parameters are kept constant: $\lambda_1^P = 150$ USD/kW and $\lambda_2^E = 5$ USD/kWh. Figure 6 shows the variation in the cost of baseload for the reference case and a 10 MW baseload. To put the numbers into perspective, the variation of cost of baseload corresponds to a share of the wind farm capital expenditure between 3% and 16%, assuming a cost of offshore wind power of 3000 USD/kW [14]. For high LTS costs, the cost of baseload is mostly driven by the STS cost (vertical contour lines) and the storage system almost entirely consists of STS (cyan region). This means that it is only relevant to consider LTS for baseload hybrid power plants below a certain cost threshold. The opposite trend can be observed for high STS

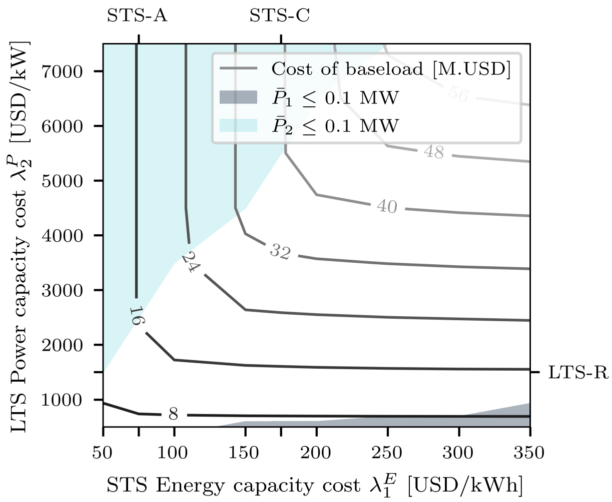

Fig. 6 Contour plot of the cost of baseload for the reference case and varying LTS and STS costs. Regions with low STS or LTS capacity in the optimal design are represented in dark blue and cyan, respectively.

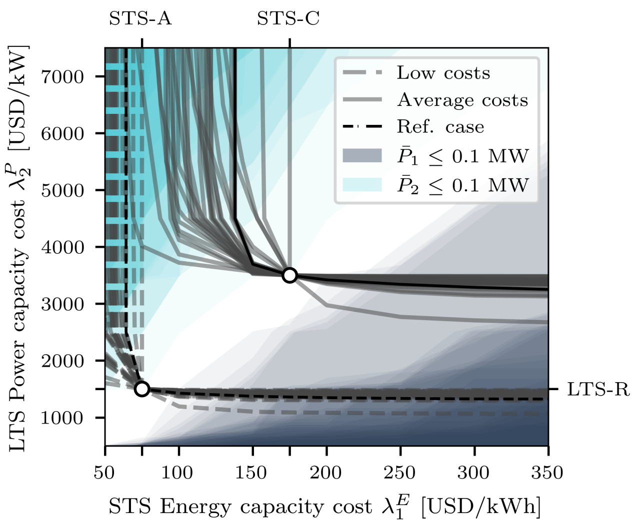

Fig. 7 Contour lines of the cost of baseload for all cases. For clarity, only two contour lines are represented for each case, passing through two pre-determined points marked as black circles and corresponding to low and average storage costs. Regions with low STS or LTS capacity are represented in dark blue and cyan, respectively. The color intensity represents the number of cases having a low STS or LTS capacity. The data for the reference case are highlighted in black.

costs. These trends can be generalized to all cases, as shown in Fig.7. Our data suggest that for expected future costs of LTS ($\lambda_2^P \leq 2000$ USD/kW), the cost of baseload is primarily driven by the LTS costs (horizontal contour line). We note that the regions where the optimal design is dominated by one type of storage are similar across cases, but not identical.

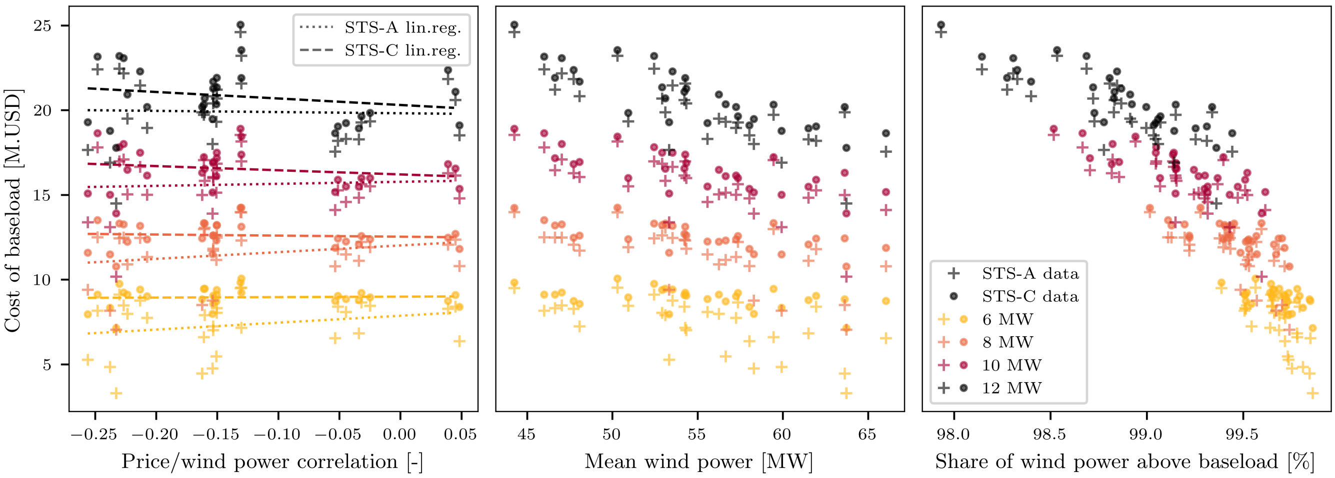

Fig. 8 Correlation between the cost of baseload and the correlation between electricity price and wind power, the mean wind power and the share of wind power produced above baseload. The dotted and dashed lines are linear regression lines based on the scatter of points for STS-A and STS-C.

4.3 Cost of baseload sensitivity to site characteristics

Finally, we study how the cost of baseload varies with the wind power production characteristics. Figure 8 shows the cost of baseload for all cases as a function of three metrics: the Pearson correlation between price and wind power, the mean wind power and the share of power produced above baseload. As expected, our data shows that the cost of baseload increases with the baseload level. However, it is weakly correlated to the price/wind correlation and the mean wind power. Despite that it is weak, we note that the correlation to the price/wind correlation consistently changes from a positive trend to a negative one for the STS-A and STS-C cost assumptions, respectively, confirming the tendency to rely more on arbitrage for the STS-A case, which pays off most for large negative correlation. Furthermore, we can observe a stronger correlation to the third metric, which represents the extent to which the baseload constraint is already covered by wind power production. These results highlight two main drivers for the cost of baseload: the baseload level and the energy to be transferred by the storage to satisfy the baseload constraint.

5 Discussion

The analysis presented in this work suggests that above a certain threshold for the STS cost, the optimal total power capacity of the storage system is approximately equal to the baseload level. Otherwise, oversizing is beneficial to increase arbitrage revenues. However, this threshold corresponds to the most optimistic cost assumptions for 2050. As such, oversizing is unlikely to be beneficial.

In addition, our results show a large sensitivity of storage sizing to the storage cost. This raises the question of the relevance of the sizing method, based on a simple but common storage model, for future project developments. The benefit of one type of storage over the other may be better accounted for if the model is able to capture the effect of storage degradation and leakage for example. Furthermore, the storage is sized using an assumption of perfect information, which may lead to unrealistic operation schedules. Finally, the objective of the sizing methodology is a metric based on an NPV formulation. While this metric has the benefit of being linear in the design variables, other metrics such as the levelized cost of energy or the ratio between NPV and total capital expenditure are often preferred for the sizing of hybrid power plants [15].

While solar PV can improve the business case of hybrid power plants, we focus on a wind-storage configuration. A preliminary analysis showed no financial benefits of adding solar PV for the considered sites with high wind and low solar resources, in accordance with the literature [16]. However, we expect our results to be valid for hybrid power plants combining wind and solar PV.

Finally, this study highlights the financial burden of baseload power production with renewable sources. While a baseload constraint may be beneficial for grid stability and reliability of supply, there is currently no such constraint imposed on renewable power plant project developers. Financial incentives could be put in place, such as subsidy premiums. However, storage system projects might be more adequately developed as independent units, as studied in [8]. In addition, a constant baseload is an abstract constraint that does not reflect well the way the energy market functions. Future work on the topic of dispatchability should be done to develop new constraints characterizing the desired flexibility of power supply.

6 Conclusions

This work highlights several trends in the design drivers for a storage system of a wind-storage hybrid power plant satisfying a constant baseload power production. We characterize the total energy and power capacity and the balance between short-term and long-term storage to minimize the financial burden of baseload production. For different offshore site locations in Northern Europe and different storage cost assumptions, the following conclusions are drawn:

- At expected future costs of long-term and short-term storage, the total power capacity of the storage system is approximately equal to the baseload power level.
- The higher the baseload level, the higher the share of long-term storage in the total energy and power capacity.
- At expected future storage costs, the cost of baseload is primarily driven by the cost of long-term storage.
- The main drivers for the cost of baseload are the baseload level and the share of renewable energy produced at a power above baseload.

7 Acknowledgements

This work is part of the Hollandse Kust Noord wind farm innovation program. Funding was provided by CrossWind C.V., and content support was provided by Shell.

8 References

[1] Dutch Minister of Economic Affairs and Climate Policy: ‘Ministerial Order for the permitting of Offshore Wind Energy Hollandse Kust (noord) wind farm site V’, 2019

[2] Brekken, T. K. A., Yokochi, A., Von Jouanne, A., et al.: ‘Optimal Energy Storage Sizing and Control for Wind Power Applications’, IEEE Trans. Sustain. Energy, 2010, p. 5547004, doi: 10.1109/TSTE.2010.2066294.

[3] Luo F., Meng K., Dong Z. Y., et al.: ‘Coordinated Operational Planning for Wind Farm With Battery Energy Storage System’, IEEE Trans. Sustain. Energy, 2015, 6, (1), pp. 253-262, doi: 10.1109/TSTE.2014.2367550.

[4] Nguyen, C.-L., Lee, H.-H. and Chun, T.-W.: ‘Cost-Optimized Battery Capacity and Short-Term Power Dispatch Control for Wind Farm’, IEEE Trans. on Ind. Applicat., 2015, 51, (1), pp. 595–606, doi: 10.1109/TIA.2014.2330073.

[5] Pfenninger S. and Keirstead J.: ‘Comparing concentrating solar and nuclear power as baseload providers using the example of South Africa’, Energy, 2015, 87, pp. 303–314, doi: 10.1016/j.energy.2015.04.077.

[6] Fasihi M. and Breyer C.: ‘Baseload electricity and hydrogen supply based on hybrid PV-wind power plants’, Journal of Cleaner Production, 2020, 243, p. 118466, doi: 10.1016/j.jclepro.2019.118466.

[7] Augustine C. and Blair N.: ‘Storage Futures Study: Storage Technology Modeling Input Data Report’, NREL/TP–5700-78694, 2021, doi: 10.2172/1785959.

[8] Dowling J. A., Rinaldi, K. Z., Ruggles, T. H., et al.: ‘Role of Long-Duration Energy Storage in Variable Renewable Electricity Systems’, Joule, 2020, 4, (9), pp. 1907–1928, doi: 10.1016/j.joule.2020.07.007.

[9] Ma, Z., Tian, T., Cui, Q., et al.: ‘Rapid sizing of a hydrogen-battery storage for an offshore wind farm using convex programming’, International Journal of Hydrogen Energy, 2023, 48, (58), pp. 21946–21958, doi: 10.1016/j.ijhydene.2023.03.037.

[10] MOSEK ApS, ‘The MOSEK Optimizer API for Python 10.1.2’, 2024, https://docs.mosek.com/latest/pythonapi/index.html

[11] Staffell I. and Green R.: ‘How does wind farm performance decline with age?’, Renewable Energy, 2014, 66, pp. 775–786, doi: 10.1016/j.renene.2013.10.041.

[12] Staffell I. and Pfenninger S.: ‘Using bias-corrected reanalysis to simulate current and future wind power output’, Energy, 2016, 114, pp. 1224–1239, doi: 10.1016/j.energy.2016.08.068.

[13] European Network of Transmission System Operators for Electricity: ‘ENTSO-E Transparency Platform’, https://transparency.entsoe.eu/dashboard/show

[14] National Renewable Energy Laboratory: ‘2022 Annual Technology Baseline’, 2022, https://atb.nrel.gov/

[15] Murcia León, J. P., Habbou, H., Friis-Møller, M., et al.: ‘HyDesign: a tool for sizing optimization for grid-connected hybrid power plants including wind, solar photovoltaic, and Li-ion batteries’, Wind Energy Science, 2023, doi: 10.5194/wes-2023-83.

[16] Murcia León, J. P. and Das, K.: ‘Profitability of hybrid power plants in Europe’, 22nd Wind and Solar Integration Workshop, Copenhagen, Denmark, 2023, pp. 302–307. doi: 10.1049/icp.2023.2752.